Carbon supplementation and bioaugmentation to improve denitrifying woodchip bioreactor performance under cold conditions

Gary W. Feyereisen*[1]
Hao Wang[2]
Ping Wang[3]
Emily L. Anderson[2]
Jeonghwan Jang[4]
Ehsan Ghane[5]
Jeffrey A. Coulter[6]
Carl J. Rosen[2]
Michael J. Sadowsky[2,3]
Satoshi Ishii[2,3]

*Corresponding Author: gary.feyereisen@usda.gov, ORCID No. 0000-0003-2785-4594

[1] USDA-ARS Soil and Water Management Research Unit, 1991 Upper Buford Circle, 439 Borlaug Hall, St. Paul, MN 55108, USA.
[2] Department of Soil, Water, and Climate, University of Minnesota, 1991 Upper Buford Circle, 439 Borlaug Hall, St. Paul, MN 55108, USA.
[3] BioTechnology Institute, University of Minnesota, 140 Gortner Lab, 1479 Gortner Ave., St. Paul, MN 55108, USA.
[4] Division of Biotechnology, Jeonbuk National University, 79 Gobong-ro, Iksan-si, Jeollabuk-do, 54596, Republic of Korea.
[5] Department of Biosystems and Agricultural Engineering, Michigan State University, 524 S. Shaw Lane, 206 Farrall Hall, East Lansing, MI 48824, USA.
[6] Department of Agronomy and Plant Genetics, University of Minnesota, 1991 Upper Buford Circle, 411 Borlaug Hall, St. Paul, MN 55108, USA.

Abbreviations:

AHRT, actual hydraulic residence time; d.l., detection limit; EPS, extracellular polymeric substance; HRT, hydraulic residence time; ITS, internal transcribed spacer; LOD, limit of detection; LOQ, limit of quantification; NRR, nitrate-N removal rate; s.e., standard error

Abstract:

Cold temperatures limit nitrate-N load reductions of woodchip bioreactors in higher-latitude climates. This two-year, on-farm (Willmar, Minnesota, USA) study was conducted to determine whether field-scale nitrate-N removal of woodchip bioreactors can be improved by the addition of cold-adapted, locally isolated bacterial denitrifying strains (bioaugmentation) or dosing with a carbon (C) source (biostimulation). In Spring 2017, biostimulation removed 66% of the nitrate-N load, compared to 21% and 18% for bioaugmentation and control, respectively. The biostimulation nitrate-N removal rate (NRR) was also significantly greater, 15.0 g N m^{-1} d^{-1}, versus 5.8 and 4.4 g N m^{-1} d^{-1}, for bioaugmentation and control, respectively. Bioclogging of the biostimulation beds limited dosing for the remainder of the experiment; NRR was greater for biostimulation in Fall 2017, but in Spring 2018 there were no differences among treatments. Carbon dosing did not increase outflow dissolved organic C concentration. The abundance of one of the inoculated strains, *Cellulomonas* sp. strain WB94, increased over time, while another, *Microvirgula aerodenitrificans* strain BE2.4, increased briefly, returning to background levels after 42 days. Eleven days after inoculation in Spring 2017, outflow nitrate-N concentrations of bioaugmentation were sporadically reduced compared to the control for two weeks but were insignificant over the study period. The study suggests that biostimulation and bioaugmentation are promising technologies to enhance nitrate removal during cold conditions. A means of controlling bioclogging is needed for biostimulation, and improved means of inoculation and maintaining abundance of introduced strains is needed for bioaugmentation. In conclusion, biostimulation showed greater potential than bioaugmentation for increasing nitrate removal in a woodchip bioreactor, whereas both methods need improvement before implementation at the field scale.

1. Introduction

Nutrient losses from agriculture degrade the quality of surface and receiving water bodies worldwide (McDowell et al., 2020). One strategy for reducing water degradation is treatment of agricultural runoff at the edge of fields. Many treatment designs use denitrification, conversion of dissolved nitrate to dinitrogen gas via microbial activity, to accomplish reductions. Designs include constructed/treatment wetlands (Bachand and Horne, 2000; Crumpton, 2001), denitrification walls (Manca et al., 2020), and woodchip denitrification beds (Schipper et al., 2010; Addy et al., 2016; Christianson et al., 2021).

Climate limitations in northern latitudes (e.g., U.S. and northern Europe) challenge the use of biological remediation of nitrate-laden tile drainage effluent due to cold springtime water temperatures (David et al., 2016; Hoover et al., 2016, Jeglot et al., 2022a). Edge-of-field nutrient reduction practices (i.e., woodchip bioreactors, saturated buffers, or constructed wetlands) rely primarily on denitrification to remove nitrate from drainage by microbial conversion to dinitrogen gas. Since denitrification rate is reduced as ambient temperature decreases (Timmermans and Van Haute, 1983), these practices are less efficient during the spring when nitrate transport is typically greatest.

Woodchip bioreactors, comprised of woodchip-filled trenches plumbed into a tile drainage system (Schipper et al., 2010), are effective at nitrate removal (Christianson et al., 2012) yet sensitive to temperature in laboratory (Feyereisen et al., 2016; Hoover et al., 2016; Nordström and Herbert, 2017) and field studies (Christianson et al., 2012; David et al., 2016). In a meta-analysis of 57 bioreactor systems, Addy et al. (2016) reported a Q_{10} (factor by which nitrate

74 removal rate changes per 10°C change) of 2.15 and urged further research at low temperatures to
75 address the problem of coincidental high flows.

76 Two approaches to enhance microbial activities *in situ* include biostimulation and
77 bioaugmentation. In biostimulation, nutrients or electron donors are added to the site or
78 environmental conditions changed (e.g., oxygen) to enhance microbial activity, whereas in
79 bioaugmentation, microorganisms capable of carrying out the desired bioremediation reaction
80 are added to the site (Tiyagi et al. 2011). Previously, Roser et al. (2018) showed in the laboratory
81 that the addition of acetate to woodchips (i.e., biostimulation) increased microbial nitrate
82 removal rate (NRR), reporting an order of magnitude improvement in NRR for acetate plus
83 woodchips versus woodchips alone at 5.5°C. We also identified and isolated denitrifiers that are
84 active at relatively low temperatures (15°C) from woodchip bioreactors (Jang et al., 2019;
85 Anderson et al., 2020), as have Jeglot et al. (2022b). Some of these microbes can breakdown
86 cellulose, a major component of woodchips, and therefore, can provide more labile carbon to the
87 environment (Jang et al., 2019). By inoculating bioreactors with cold-adapted denitrifiers, it
88 would be possible to enhance nitrate removal at cold conditions. However, biostimulation and
89 bioaugmentation have not been tested concurrently in field-scale woodchip bioreactors and may
90 be beneficial to enhance nitrate removal from water.

91 The focus of this study was to improve nutrient reduction efforts in colder climates by
92 demonstrating, evaluating, and improving upon the effectiveness of woodchip bioreactors for
93 treating agricultural subsurface tile drainage. The study objective was to compare nitrate-N
94 removal in field pilot-scale woodchip bioreactors by inoculating with selected cold-adapted
95 denitrifiers (bioaugmentation) or by supplementing with readily available carbon (C)
96 (biostimulation). The hypotheses were that i) addition of selected microorganisms will enhance

97 nitrate-N removal, and ii) addition of C in the form of acetate will enhance nitrate removal [due
98 to stimulation of microbial denitrification].

99 2. Materials and methods

100 *2.1 Site and Experimental Setup*

101 A replicated woodchip bioreactor field study was conducted on a private farm near Willmar,
102 Minnesota, USA, from Fall 2016 through Spring 2018. Inflow originated from subsurface
103 drainage discharge from adjacent fields cropped with maize (*Zea mays*) harvested for grain.
104 Treatments included a control (Control), bioaugmentation (BioAug) with denitrifiers selected for
105 low-temperature denitrification performance, and biostimulation (BioStim) with dosing of
106 acetate. Water flow, nitrogen (N), phosphorus (P), and dissolved carbon (C) were measured
107 throughout the drainage year; focused treatment campaigns were conducted in Fall 2016, Spring
108 2017, Fall 2017, and Spring 2018.

109 In October 2014, a four-year old plastic-lined woodchip bioreactor (1.7-m wide by106-m long)
110 was reconstructed into eight replicated bioreactor beds (1.7-m wide by 11.6-m long) (Fig. S1)
111 (Ghane et al., 2018; Ghane et al., 2019). The soil cover (0.75±0.15 m) was removed from the top
112 of the woodchip bed where the inlets and outlets of the reconstructed beds were to be located.
113 Woodchips were excavated and adjacent beds were separated using a 2-m wide compacted soil
114 berm, with rigid plastic sheets (1.3-cm thick) inserted before and after the soil berms to prevent
115 water movement between beds. A 0.51-mm thick liner was placed in the beds, inlet and outlet
116 manifolds were installed, the ends of the beds refilled with the exhumed woodchips, and the soil
117 cover replaced. PVC pipes (15-cm inside dia.) were vertically inserted to the bottom of the beds

60 cm from the inlet (Port 2), at approximately one-third (Port 3) and two-thirds (Port 4) the length of the bed, and 60 cm from the outlet (Port 5) (Ghane et al., 2019). Baskets containing approximately 30 woodchip balls (sediment sock material filled with approximately 100 g of woodchips, 7–8-cm dia.; Fig. S2) for sample collection were inserted into the vertical PVC pipes.

Drainage discharge from the adjacent fields flowed into a vertical pit from which the water was pumped into an aboveground, insulated, 11.4-m^3 constant-head supply tank. From the supply tank, water flowed by gravity to a PVC manifold and through 3.8-cm diameter PVC pipes to each bed with the flow rate for each bed independently adjustable (1.9-cm manual gate valve). Outflow from the bed outlets was pumped by sump pumps in 26-L buckets. Paddlewheel flow sensors were used to measure flow rate into (inflow) and out of (outflow) each bed. Pressure transducers measured bed water level and temperature; temperature within the supply tank was also monitored. Sensors were connected to several dataloggers, which were connected by radio to a base station with a modem.

Construction and troubleshooting of the beds, piping, and instrumentation was completed by summer's end 2016. Four experimental campaigns were conducted: Fall 2016, Spring 2017, Fall 2017, and Spring 2018. Each campaign consisted of inoculation of the BioAug beds with selected denitrifiers and introduction of acetate into the BioStim beds. Physical and chemical properties of the woodchips in each bioreactor bed were determined to be similar for bed numbers 3 through 8 (counting from the inlet end of the original bed) (Ghane et al., 2018). Therefore, these six beds were used to conduct the replicated experiment to explore the nutrient removal performance of the experimental treatments.

2.2 Treatments

The following replicated (n = 2) treatments were established: Control - woodchip beds left as is; BioAug - addition of selected cold-tolerant denitrifying bacteria (see *2.2.1* below); BioStim - addition of acetate, a readily available carbon source. Bioreactor bed numbers 3 through 8 were randomized for the Fall 2016 experimental campaign. Since there were neither microbial nor nutrient removal treatment differences during Fall 2016, beginning in Spring 2017 the beds were blocked based on landscape position and randomized within each block. The blocks consisted of numbers 3 through 5, and numbers 6 through 8. The higher numbered beds (6 through 8) were further from the supply tank and at a lower elevation in the landscape and thus more likely to be influenced by high ground water table after precipitation events.

2.2.1 Bioaugmentation: Strains used

Denitrifying and nitrate-reducing bacteria were isolated from woodchip bioreactors as described previously (Jang et al., 2019; Anderson et al., 2020). Strains were selected based on their nitrate reduction capabilities at relatively low-temperature conditions (15°C). As a result, four strains were selected for bioaugmentation: *Bacillus pseudomycoides* strain I32, *Cellulomonas cellasea* strain WB94, *Microvirgula aerodenitrificans* strain BE2.4, *Lelliottia amnigena* strain BB2.1 (Table S1). However, in late 2017, two of the inoculated strains, *Bacillus pseudomycoides* strain I32 and *Lelliottia amnigena* strain BB2.1, were identified as non-denitrifiers. They reduced nitrate to ammonium, not to N_2 gas (Anderson et al., 2020). *Cellulomonas cellasea* strain WB94 and *Microvirgula aerodenitrificans* strain BE2.4 were confirmed as denitrifiers. Furthermore, strain WB94 was identified as a cellulose degrader.

Inoculation and initiation of biostimulation occurred as follows: Fall 2016, 20 October (*Bacillus pseudomycoides* I32); Spring 2017, 8 May (*Cellulomonas* sp. strain WB94); Fall 2017, 17 and 31

October (*Microvirgula* sp. strain BE2.4, *Lelliottia* sp. strain BB2.1) (Table S1); Spring 2018, 2 and 16 2018 (*Microvirgula* sp. strain BE2.4), and 30 May (*Microvirgula* sp. strain BE2.4, *Cellulomonas* sp. Strain WB94). The strains were aerobically grown in R2A medium (10L) supplemented with 5 mM nitrate and 10 mM acetate at 30°C, except for *Bacillus pseudomycoides* strain I32, for which nutrient broth was used. Cells were pelleted by centrifugation, re-suspended with 0.85% NaCl, and kept at refrigerated temperature until inoculated (usually <24 h). Suspended cells were poured into the inflow stream of the BioAug treatment beds. In Fall 2017, bed flow rate was reduced in the BioAug treatment beds and left low for one week after the inoculation to improve the effectiveness of BioAug treatment.

2.2.2 Biostimulation

Sodium acetate solution was stored in 200-L drums in the small storage huts at the head ends of the two biostimulation treatment beds. The solution was delivered into the inflow stream with a peristaltic pump controlled by a datalogger. Concentrations, duty cycles, and flow rates are shown in Table S2. Changes were made throughout the project to optimize nitrate removal and avoid bioclogging.

To minimize cost and potential for bioclogging, the C:N ratio for the Fall 2016 campaign was designed so that acetate would provide only a portion of the electron donors required for complete denitrification. Since the onflow nitrate-N concentration for Fall 2016 was greater than estimated, the actual C:N ratio was even less than anticipated. No improvements were noted in effluent nitrate-N concentrations, nitrate-N load removal, or NRR, so in Spring 2017 the C:N ratio was increased to values near those used in previous laboratory testing (Roser et al., 2018). Five weeks after initiation of acetate addition, bioclogging of the BioStim beds occurred by

184 excess extracellular polymeric substance (EPS) production, reducing flows. Pressure transducers,
185 connected to data loggers, were installed in the inlet pipes to monitor clogging and subsequent
186 high inlet water level. From that time until the end of the experiments, addition of acetate to the
187 beds was halted when the water level of the inlet pipe rose, which indicated reduced flows, and
188 restarted when the water level dropped. In Spring 2018, inflow rates were increased in the
189 BioStim beds to reduce bioclogging.

190 *2.3 Actual Hydraulic Residence Time*

191 The actual hydraulic residence time (AHRT) was determined using in-situ effective porosity of
192 the woodchip media (e_v) for each bed (Ghane et al., 2016; Ghane et al., 2019). Briefly, bromide
193 tracer tests were conducted on each bed to determine the mean tracer residence time ($\bar{t}$). The in-
194 situ effective porosity (n_e) was calculated as:

195 $$n_e = \frac{QT_{avg}\,\bar{t}}{V_s} \quad (1)$$

196 where QT_{avg} was the average flow rate of the bed inflow and outflow during the bromide tracer
197 test, ($\bar{t}$) was the mean tracer time determined from the bromide tracer test, and V_s was the
198 saturated volume of the woodchip bed. Then, AHRT was calculated as:

199 $$AHRT = \frac{V_s\,n_e}{QE_{avg}} \quad (2)$$

200 Where QE_{avg} was the average daily flow rate of the bed inflow and outflow during the current
201 research experiments and V_s and n_e were defined as above.

202 *2.4 Experimental Dates and Water Sampling*

203 *2.4.1 Automated sampling regime*

Water samples for nutrient analysis for Fall 2016 were collected with automated water samplers (ISCO 6712, Teledyne ISCO, Lincoln, NE, USA) installed in small storage huts at the supply tank and the outlet of each bed. Power was supplied by 12-v dc deep cycle batteries recharged by solar panels. A time-based composite sampling strategy was used for the inflow and outflow. The automated sampler at the supply tank was programmed to pump 160-mL aliquots at 4-hour intervals daily into a 1-L bottle containing 1.25 mL concentrated H_2SO_4 (Cleresci et al., 1998). The water was pumped from near the level of the tank outlet. For the Fall 2016 campaign, the same sampling regime (one 1-L bottle per day) was used for outflow sampling of all the beds. To reduce the sample handling and analysis load, outflow sampling for Spring and Fall 2017 was reduced to one 1-L bottle each 3 days (80-mL subsamples at 6-hour intervals) and for Spring 2018 changed to one 1-L bottle each 2 days (80-mL subsamples at 4-hour intervals). The 1-L bottles were collected weekly, placed in coolers, transported to St. Paul, Minnesota, and stored in a cooler (4°C). Filtered (0.45 μm) and unfiltered samples were prepared for analysis and archived (-20°C).

2.4.2 Weekly manual sampling regime

Water samples for DOC analysis were manually collected on a weekly basis during the Spring 2017 and Fall 2017 campaigns, and less frequently during Spring 2018 (Table S3). Samples were collected in 250 mL polyethylene bottles from the supply tank outlet and from each bioreactor outflow, filtered (0.45 mm) and transferred to 20-mL scintillation vials, placed in a cooler on ice, returned to St. Paul, Minnesota, USA, and frozen until analysis.

2.4.3 Port sampling regime

On 8 and 15 May, 31 October, and 14 and 28 October 2017, and 2, 16, 30 May 2018 woodchip balls from Ports 2, 3, 4, and 5, and water samples from these Ports plus the inlets and outlets of each bed were collected (Wang et al., 2022). Woodchip balls were immediately placed on ice, transported to St. Paul, MN, and stored at -20°C until processed (see *2.6* below). Beginning with the Control beds, water was pumped from the outlet sump, 4 ports from the outlet to the inlet (Ports 5 to 2), and finally from the inlet with a peristaltic pump connected to a 10-mm diameter polycarbonate tube inserted into the ports to a depth of approximately 5 cm from the bottom of the bed. Water for nutrient analysis was collected in 250 mL polyethylene bottles and processed on site. Filtered (0.45 mm) and unfiltered samples (17 mL) were poured into scintillation vials, acidified per sample plan, placed in iced coolers, transported to St. Paul, and stored (-20°C) until analyzed for nitrate-N and DOC (see *2.5* below). At each port, after water was sampled, dissolved oxygen (DO) and pH were measured by continuously pumping water into the bottom of a polyethylene container and allowing the water to upwell around a multiparameter water sonde (YSI Professional Plus, YSI Instruments, Yellow Springs, OH, USA).

2.5 Water Analysis

Filtered samples were analyzed by flow-injection colorimetry (Lachat QuikChem 8500, Hach Co.) for nitrate-N concentration (NO_3-N + NO_2-N) (method number 10-107-04-1-A) and ammonium-N concentration (method number 10-107-06-2-A). Unfiltered samples for total-P (TP) concentration determination were digested (alkaline persulfate; Patton and Kryskalla, 2003) prior to analysis by the reactive P method number 10-115-01-1-A for TP. Filtered samples were analyzed for dissolved C (DC) concentration by combustion (vario TOC select, Elementar Analysensysteme, Gmbh, Hanau, Germany). Dissolved inorganic C (DIC) concentration was determined by bubbling phosphoric acid through the sample and analyzing released CO_2 with an

infrared detector. Dissolved organic C (DOC) concentration was determined by difference, DC minus DIC.

Nitrate-N and total-P loads into and out of each bioreactor bed were calculated by multiplying the concentrations by the outflow volume during collection of the sample bottle using the midpoint in time as demarcation between bottles. Load reductions were calculated as a percentage: the difference in inflow and outflow load, divided by the inflow load. The NRR (units of g N $m^{-3}d^{-1}$) was calculated as the difference in inflow and outflow load, divided by time and divided by the wetted volume of the bed as determined by Ghane et al., 2019 (Schipper et al., 2010).

2.6 DNA extraction of woodchip samples

The woodchip balls collected from the woodchip bioreactor beds were used for DNA extraction and downstream analysis for microbial community composition. The woodchip balls collected from the field were first removed from the -20°C freezer and left at room temperature for 40 minutes before processing. This process allowed the woodchip balls to thaw. Then, 25 g of woodchip were put into a 160 mL wide mouth milk dilution bottle (Corning) containing 100 mL of PBS-gelatin buffer and 25 g glass beads (5 mm). Then the milk bottles were placed on a shaker and shaken for 30 minutes. The PBS-gelatin buffer in the milk bottle was then transferred to a 50 mL falcon tube (Thermo Scientific Cat# 339652) and centrifuged at 10,000 rpm (11,953 RCF) for 15 minutes at 4°C. After the centrifugation, the supernatant was discarded, and this process was repeated until all the PBS-gelatin buffer from the milk bottle was transferred and centrifuged. The bacterial pellet from the woodchip was then weighed and stored in a 2-ml

centrifuge tube at -80°C until further processing. A total of 213 woodchip samples were collected, and 209 samples were processed and later used for DNA extraction. Four samples were discarded due to mislabeling. The list of samples collected was shown in Wang et al. (2022).

The PowerSoil DNA extraction kit (Qiagen) was used to extract DNA from the bacterial pellet washed off from the woodchips. The extraction was done using the QIAcube Connect automated system (Qiagen) following the manufacture's protocol, with the exception that 0.5 g of the bacterial pellet was used for the extraction instead of 0.25 g of soil. The DNA elution was diluted 10-fold and stored in the -80°C freezer. The quality of DNA was verified with qPCR targeting the 16S rRNA gene as described by Jang et al. (2019).

2.7 Quantification of inoculated strains by quantitative PCR

Quantitative PCR (qPCR) was used to quantify the abundances of inoculated denitrifying strains (*Cellulomonas* sp. strain WB94 and *Microvirgula aerodenitrificans* strain BE2.4). Strain-specific TaqMan probes and primers were designed based on the internal transcribed spacer (ITS) region between the 16S and 23S rRNA genes. The ITS sequences were retrieved from the genome sequences available in the GenBank database including those for strain WB94 (GenBank accession*:* QEES00000000) and strain BE2.4 (GenBank accession*:* NZ_CP028519.1). Molecular Evolutionary Genetics Analysis (MEGA) software was used to align these sequences and identify the region unique to *Cellulomonas* strain WB94. The unique ITS region was used to design qPCR assays by using Roche ProbeFinder version 2.53. For *Microvirgula* sp. strain BE2.4, the ITS region specific to this strain could not be identified because only one ITS sequence was available on the GenBank database. We therefore used the entire ITS sequence of

strain BE2.4 to design strain BE2.4-specific qPCR assay. The qPCR assays designed are summarized in Table S4.

The qPCR reaction mixture (10 µl) contained: 1x SsoAdvanced Universal Probe Supermix (Bio-Rad), 800 µM each primer, 100 µM probe, and 1 µl template DNA. The qPCR was conducted using the StepOnePlus Real-Time PCR system (Applied Biosystems) with the following thermal conditions: 3 minutes at 95°C, followed by 40 cycles of 5 seconds at 95°C and 30 seconds at 60°C. Threshold cycle (Ct) values were determined using StepOnePlus v2.3. Standard curves were generated by plotting the Ct values vs. the abundance of standard DNA (i.e., serial dilutions of the genomic DNA from target bacteria). The r^2 values of the standard curves were all >0.99; the average qPCR efficiency for strain WB94 was 94.72% and for strain BE2.4 was 103.18%. Target gene abundances in the woodchip samples were determined based on the Ct values by using the standard curves (Ishii et al., 2013). For samples that showed below the limit of quantification (LOQ; 5.8 and 1.0 copies/µl for *Cellulomonas* sp. strain WB94 and *Microvirgula aerodenitrificans* strain BE2.4, respectively), limits of detection (LOD)/2 were assigned as recommended by Hites (2019).

2.8 Statistical analysis

The automated sample data were paired by bed outflow sample; each sample represented 1 d for Fall 2016, 3 d for Spring and Fall 2017, and 2 d for Spring 2018. In 2017 and 2018, the daily inflow concentrations and loads were flow averaged to match the period of the outflow samples. The data were vetted as follows. Sample dates with a missing treatment(s) due to equipment failure or anomalies due to precipitation events or high groundwater levels were excluded from analysis. The number of automated samples used for analysis of treatment effects for Fall 2016,

Spring 2017, Fall 2017, and Spring 2018 were 25, 19, 13, and 23 respectively (Table S5). Concentrations of ammonium and phosphorus below the detection limit (d.l.), 0.005 mg N L^{-1} and 0.003 mg P L^{-1}, respectively, were replaced with (d.l.)/2.

Hydraulic Residence Time, AHRT, nitrate-N, ammonium-N, and TP concentrations, nitrate-N and TP loads and load reductions as a percentage for Fall 2016, Spring 2017, Fall 2017, and Spring 2018, along with weekly DOC outflow concentrations for Spring 2017 and Fall 2017 were analyzed using the MIXED procedure of SAS (SAS Institute, 2016) at $P \leq 0.10$. Treatment was considered a fixed effect, sampling date was considered a fixed effect and repeated measurement, and block and interactions with block were considered random effects. Data were analyzed separately by campaign (i.e., Fall 2016, Spring 2017, Fall 2017, and Spring 2018) due to differences in sampling dates. Means were compared with pairwise *t*-tests at $P \leq 0.10$ using the PDIFF option of the MIXED procedure of SAS.

To determine whether the bioreactors were net consumers or producers of ammonium-N or DOC throughout the campaigns and immediately following inoculation, sample date inflow concentrations were subtracted from average outflow concentrations (automated samples) for these two analytes across treatments for Spring 2017 and Fall 2017, and Spring 2018. This difference in ammonium-N or DOC concentration, "Delta-NH_4-N" and "Delta-DOC" herein, was tested to determine whether it was significantly different from zero using *t*-tests at $P \leq 0.10$ via the LSMEANS option of the MIXED procedure of SAS.

3. Results

3.1 Experimental conditions

335 Averaged AHRT (across dates) was similar among treatments for Fall 2016, Spring 2017, and
336 Fall 2017, ranging from 9.8 to 11.7, 10.2 to 11.2, and 10.0 to 11.2 h (P = 0.11, 0.87, and 0.58)
337 for these campaigns, respectively (Table S6). For Spring 2018, average AHRT was similar for
338 Control and Biostim, 11.5 and 11.0 h, respectively, and was different for BioStim (5.2 h) since
339 flow rates were increased (Table S6). Daily average inflow temperatures for the Fall 2016,
340 Spring 2017, and Fall 2017, and Spring 2018 experiments ranged from 13.4 to 11.6, 6.9 to 13.2,
341 13.2 to 8.4ºC, and 3.4 to 12.5°C, respectively (Fig. S3). For all treatments, average DO
342 concentrations dropped to ≤0.47 mg O L^{-1} at Port 3, one-third of the distance from the inlet to the
343 outlet, indicating conditions supportive of denitrification (Fig. 1).

344 *3.2 Nitrate-N load reduction and nitrate removal rate*

345 There were no significant differences among treatments for outflow nitrate-N concentration,
346 nitrate-N load reduction, or NRR for Fall 2016 (Table 1, Fig. 2a; P = 0.11, 0.58, and 0.59,
347 respectively). Inflow concentration averaged 19.4 mg N L^{-1} (range 18.2–20.6) and the Control,
348 BioAug, and BioStim concentrations averaged 14.4, 14.9, and 14.9 mg N L^{-1}, respectively. The
349 average percentage concentration reductions were 26, 23, and 23%, for these respective
350 treatments, and the average NRRs were 5.9, 6.6, and 6.4 mg N m^{-3} d^{-1}, respectively.

351 During the Spring 2017 and Fall 2017 campaigns, inflow concentrations averaged 17.8 mg N L^{-1}
352 (range 12.9–20.5) and 14.5 mg N L^{-1} (range 14.0–15.8), respectively (Fig. 2b, 2c). Treatment
353 outflow nitrate-N concentrations for Spring 2017 and Fall 2017 were significantly lower for
354 BioStim relative to Control and BioAug (Table 1; P < 0.001 and 0.006, respectively).
355 Consequently, for Spring 2017 nitrate-N load removal was greater for BioStim than for Control
356 and BioAug, 65, 17, and 21%, respectively (P = 0.004), and for Fall 2017, 31, 20, and 16%,

357 respectively (Table 1; $P = 0.017$). Nitrate removal rates were also greater for BioStim for Spring
358 and Fall 2017: 15.0, 4.4 and 5.8 mg N m^{-3} d^{-1} ($P = 0.029$), for Spring 2017 and 5.6, 4.1, and 3.9
359 mg N m^{-3} d^{-1} ($P = 0.095$), for Fall 2017 for BioStim, Control, and BioAug, respectively (Table
360 1). The greater NRR for BioStim in 2017 corresponded to lower port nitrate-N concentrations
361 from Port 3 to the outlet (Fig. 3).

362 For the Spring 2018 campaign inflow concentrations averaged 13.8 mg N L^{-1} (range 8.8–17.8)
363 (Fig. 2d). Outflow nitrate-N concentrations were significantly different with Control < BioAug <
364 BioStim, (Table 1, $P = 0.036$). A 63-mm precipitation event on 11 June 2018 resulted in loss of
365 two sampling dates due to rise in the local water table and appeared to have caused a shift in
366 outflow nitrate-N concentrations among treatments (Fig. 2d, S3). Nitrate-N load reduction was
367 also different among treatments with Control > BioAug > BioStim (Table 1, $P = 0.039$).
368 However, NRRs were insignificant among treatments–4.93, 4.09, and 4.86 mg N L^{-1} for Control,
369 BioAug, and BioStim, respectively (Table 1, $P = 0.54$).

370 *3.3 Ammonium concentrations and dynamics*

371 Inflow ammonium-N concentrations ranged from below detection limit (0.005 mg N L-1) for
372 each campaign to 0.107 mg N L^{-1} for Spring 2017, 0.139 mg N L^{-1} for Fall 2017, and 0.021 mg
373 N L^{-1} for Spring 2018 (Fig. 4). Ammonium-N inflow concentrations increased throughout Spring
374 2017 (7 May to 9 July. $P = 0.04$) and decreased throughout Fall 2017 (28 Oct to 4 Dec, $P =$
375 0.02). There were no significant differences in outlet ammonium-N or Delta-NH_4-N (outflow
376 minus inflow) concentrations among treatments for the Spring 2017, Fall 2017, or Spring 2018
377 campaigns ($P = 0.73$, 0.87, and 0.72, respectively). Outflow ammonium-N concentrations
378 averaged across treatments by date were significantly different for the Spring 2017, Fall 2017,

and Spring 2018 campaigns (Fig. 4; $P = 0.022$, 0.073, and <0.001, respectively) with a trend of increasing concentration during Spring 2017 ($P < 0.001$) and decreasing concentration during Fall 2017 ($P = 0.003$), following the inflow concentration trends.

Delta-NH4-N was not different from zero for any of the treatments for Spring 2017, Fall 2017, or Spring 2018. However, when averaged across treatments Delta-NH_4-N was greater than zero (net production) for 15 of the 19 Spring 2017 sampling dates, five of the 11 Fall 2017 dates, and nine of the 23 Spring 2018 dates (Table S7). Delta-NH_4-N was significantly less than zero (net consumption) for two dates in Fall 2017 (Table S7).

3.4 Total phosphorus concentration and load reduction

Inflow TP concentrations averaged 0.117, 0.087, 0.072, and 0.086 mg P L^{-1} for Fall 2016, Spring 2017, Fall 2017, and Spring 2018, respectively (Fig. 5). Outflow TP concentrations averaged (ranged) 0.021 (0.002–0.092), 0.032 (0.008–0.098), 0.018 (0.010–0.048), and 0.033 (0.016–0.052) mg P L^{-1} over the same periods, respectively. Outflow concentrations were consistently below inflow concentrations except for two samplings of the BioAug treatment following a period of interrupted flow in Fall 2017 due to a pumping issue in Fall 2017 (data not shown). During Fall 2017, outflow TP concentrations for BioStim were significantly less than for BioAug or Control (Table 1, $P = 0.04$). Consequently, TP load reduction was greater for BioStim in Fall 2017 than for BioAug and Control, 80.4% versus 72.9 and 70.6%, respectively (Table 1). There were no differences in TP outflow concentrations or load reductions among treatments for Fall 2016, Spring 2017, or Spring 2018.

3.5 Dissolved organic carbon concentrations and net production

For Spring 2017 weekly outflow DOC concentrations were similar by treatment ($P = 0.58$). Dissolved organic C concentrations across treatments ranged from 3.9 to 11.0 mg C L^{-1}, and differences among dates were insignificant (Table 2). Fall 2017 DOC concentrations by treatment were also insignificant ($P = 0.50$). Averaged across treatments, Fall 2017 outflow DOC concentrations were in a tight range for the four sampling dates, 5.2 to 5.7 mg C L^{-1}, yet there were significant differences among dates ($P < 0.016$, Table 2). Similar to Fall 2017, there were no treatment differences in outflow DOC concentrations for Spring 2018 ($P = 0.66$), but there were differences among dates ($P < 0.001$, Table 2), and there was a treatment by date interaction ($P = 0.02$).

Delta-DOC concentration (averaged outflow concentration minus inflow concentration) was different from zero (greater than) for one of the nine Spring 2017 sampling dates, all four Fall 2017 sampling dates, and two of the three Spring 2018 sampling dates (Table 2). Thus, significantly different net DOC production occurred on less than half the sampling dates (7 of 16). For Spring 2017, Delta-DOC values included positive and negative values; for Fall 2017 and Spring 2018 Delta-DOC was positive, indicating consistent, although minimal, net DOC export. Delta-DOC concentrations for the Control in Fall 2017 were significantly different from zero as were all three treatments in Spring 2018 (Table S8).

3.6 Quantification of inoculated strains

Cellulomonas sp. strain WB94 was inoculated in Spring 2017 (8 May 2017) and Spring 2018 (30 May 2018) to the BioAug beds. Woodchip samples were collected one week after the inoculation in Spring 2017 (15 May 2017) and 0 and 21 days after the inoculation in Spring 2018 (30 May 2018 and 20 June 2018) and used for qPCR analyses. This strain was not inoculated in our Fall

2017 campaign, but woodchip samples collected in Fall 2017 were also used for qPCR targeting strain WB94 to analyze the background population.

Cellulomonas sp. strain WB94 was not detected in the samples collected in Spring 2017; however, it was detected in 75% of samples collected from the BioAug beds on the date of inoculation in Spring 2018. Interestingly, this strain was also detected in 75% and 63% of samples from the BioStim and Control beds, respectively. The mean abundance of strain WB94 in the BioAug, BioStim, and Control beds was 4.45, 4.38, and 3.81 log copies per 25 g woodchip, respectively, and was significantly different by treatment ($P < 0.10$). *Cellulomonas* sp. strain WB94 was also detected in 75% and 71% of samples collected from the BioAug and BioStim beds, respectively, 21 days after the inoculation (20 June 2018), whereas the bacterium was detected in only 25% of samples collected from the Control beds.

Overall, strain WB94 was found in 40%, 51%, and 64% of the samples collected in Spring 2017, Fall 2017, and Spring 2018, respectively. The abundance of *Cellulomonas* sp. strain WB94 increased over time (i.e., from 2017 to 2018) ($P < 0.01$) with an average log copy number of 3.92, 3.84, and 4.32 for Spring 2017, Fall 2017, and Spring 2018 respectively. Based on the post-hoc Tukey HSD test, there was a difference between Spring 2018 and Spring 2017 samples as well as between Spring 2018 and Fall 2017 samples. However, there was no difference between the Spring 2017 and Fall 2017 samples. This suggests that the abundance of *Cellulomonas* sp. strain WB94 significantly increased over winter 2017.

Another cold-adapted denitrifier, *Microvirgula aerodenitrificans* strain BE2.4, was inoculated in Fall 2017 (17 October 2017) and Spring 2018 (2 May, 16 May, and 30 May 2018). In Fall 2017, strain BE2.4 was found in 63%, 0%, and 25% of samples collected from the BioAug, BioStim,

and Control beds, respectively, 14-day after the inoculation (31 October 2017). Interestingly, strain BE2.4 was positive in only 25% of samples collected from the BioAug beds 28 days after the inoculation and 38% of samples collected from the same beds 42 days after the inoculation (28 November 2017). The abundance of strain BE2.4 was not significantly different ($P = 0.71$) among the woodchip samples collected from the BioAug, BioStim, and Control beds 42 days after the inoculation.

Microvirgula aerodenitrificans strain BE2.4 was inoculated three times in Spring 2018 (2 May, 16 May, and 30 May 2018). Strain BE2.4 was positive in 75%, 25%, and 38% of samples collected on 20 June 2018 from the BioAug, BioStim, and Control beds, respectively, 21 days after the third inoculation. The mean abundances of strain BE2.4 in the BioAug, BioStim, and Control beds were 3.66, 2.79, and 3.03, respectively, and were significantly different by treatment ($P < 0.05$). Based on the post-hoc Tukey HSD test, abundance of strain BE2.4 was significantly different between samples collected from the BioStim beds and those from the BioAug beds ($P = 0.027$). But no difference was seen between the BioStim and Control beds ($P = 0.71$) and between BioAug and Control beds ($P = 0.11$).

4. Discussion

The transport of N, in the nitrate form, and P from subsurface-drained agricultural fields contributes to degradation of water quality in receiving water bodies. Losses are exacerbated in latitudes with cold seasons during which plant uptake, evapotranspiration, and microbial activity are reduced. One strategy for lowering these losses is treatment of tile effluents at the edge-of-field using woodchip bioreactors, in which nitrate-N is converted to dinitrogen gas via the process of microbial denitrification. This process is temperature sensitive (Q_{10} of 2 to 3), and at

466 the time of year when N losses tend to be greater, nitrate-N removal rates tend to be lower.
467 Strategies to improve cold performance of denitrifying woodchip bioreactors include augmenting
468 the microbial community with strains selected for cold performance and stimulating
469 denitrification with a source of readily available C. The purpose of the research reported herein
470 was to evaluate the N removal performance of these two strategies at a pilot scale in a real-world
471 environment.

472 An important finding of this research was the field demonstration of significant improvement in
473 NRR by dosing a woodchip bioreactor bed with a readily available C source (i.e.,
474 biostimulation). During Spring 2017, nitrate-N removal was nearly complete (4-week average of
475 97.3%) prior to onset of bioclogging issues (see second paragraph below). Water temperatures
476 during this period ranged from 6.9 to 10.3°C (Fig. S3). Even though NRRs appeared to be nitrate
477 limited during this period (Fig. 1b), they were greater (4-week average of 22.9 g N m^{-3} d^{-1}) than
478 for woodchip media reported for similar temperatures (<8 g N m^{-3} d^{-1}) in a meta-analysis of 15
479 bioreactor bed studies (Addy et al., 2016). In an earlier review of bioreactor studies, Schipper et
480 al. (2010) reported a range of NRR of 2 to 22 g N m^{-3} d^{-1} from temperatures ranging from 2 to
481 20°C, with greater rates corresponding to higher temperatures. The most recent review of peer-
482 reviewed bioreactor studies since Addy et al. (2016) reports a median of 5.1 g N m^{-3} d^{-1}, with
483 95% of NRRs <15 g N m^{-3} d^{-1} (Christianson et al., 2021).

484 Dosing the woodchip bed with C improved the NRR yet did not increase outflow DOC
485 concentrations over the Control or BioAug treatments. This finding suggests that microbial
486 processes in the beds at the flow and temperature of this experiment were sufficiently robust to
487 prevent unintended release of DOC when dosing with readily available carbon. The woodchip
488 media in these beds were well used, as they were in their sixth and seventh years of operation

during these experiments. In accord with what others have found after the initial half year to one year of operation, DOC release was modest. (Schipper et al., 2010; David et al., 2016). Warneke et al. (2011) reported slight consumption of DOC over a year's sampling of a field woodchip bioreactor receiving greenhouse effluent, with temperatures ranging from 15.5 to 23.7°C. In that study, DOC concentration increased along the bed length during the coolest sampling date.

Bioclogging of woodchip bioreactor beds dosed with C is a challenging problem that must be addressed to realize the benefits of significantly improved NRR. The issue of woodchip bed bioclogging is not often raised in the woodchip bioreactor literature, although David et al. (2016) surmised it may have caused decreasing porosity resulting in multiple specific discharge values for a given hydraulic gradient. In the current study, the addition of C stimulated excess EPS production, and temperature may have played a role given that bioclogging began when inflow temperatures exceeded 11°C. After the onset of bioclogging, obstruction of flow plagued the experiment even after a resting period of no flow during the no-flow months of July and August 2017. During this period, full oxygenation of the beds may have been hindered by the design of the outlet pumping system–water table depth remained to the rim of the 26-L buckets set at the bed bottom.

An attempt to reduce bioclogging by increasing flow rate in the BioStim beds in Spring 2018 was unsuccessful. When flow became restricted, C dosing automatically halted. The outcome was that little C was added during Spring 2018, and the average NRR for BioStim over the campaign was the same as for Control. There were four sampling dates in May 2018 for which NRR for BioStim was greater than for Control; however, as in the previous year, as the experiment progressed and water temperature increased, bioclogging hindered flow and therefore nitrate-N removal.

In the related field of constructed wetlands for wastewater treatment, researchers' suggestions for addressing bioclogging that have merit for woodchip bioreactors include: selecting filter media with coarse fractions (Suliman et al., 2006) packed optimally (Song et al., 2015), oxygenating the media by periodic draining ("resting") (Nivala et al., 2012), treating the influent (Guofen et al., 2010; Ping, et al., 2018; Cao et al., 2021), or disrupting bacterial quorum sensing (Shi et al., 2017). In addition to intermittent operation, Nivala et al. (2012) suggest inclusion of multiple inlet manifolds in bed design. Maxwell et al. (2019) have shown that short periods of draining/resting for woodchip bioreactor columns enhances NRR and increases overall N load removal despite the "down" time, a consideration if intermittent operation for C dosing of woodchips beds proves necessary to overcome bioclogging.

Another important finding of this research was the field demonstration that strain abundance and NRR were somewhat increased after inoculation, although the positive effects were short lived. For a period of 11 to 26 days after the Spring 2017 inoculation, the average outflow nitrate-N concentration of the BioAug beds was significantly less than Control for four sampling dates and NRR was significantly greater for two sampling dates (Fig. 2b). At day 11, outflow nitrate-N concentration was similar for both BioAug beds (i.e., small s.e.); however, for the next two weeks the concentrations were inconsistent between the beds as shown by the large s.e.s. The performance improvement attributable to inoculation of cold-adapted denitrifiers was not observed in any of the other campaigns.

We inoculated *Cellulomonas* sp. strain WB94, a cold-adapted and cellulose-degrading bacterium (Jang et al., 2019) and *Microvirgula aerodenitrificans* strain BE2.4, a cold-adapted and aerobic denitrifying bacterium (Anderson et al., 2020) to the bioreactors. Based on our qPCR analysis, the abundance of *Cellulomonas* sp. strain WB94 increased over time in the woodchip beds. Since

535 this strain and other *Cellulomonas* species can degrade cellulose and other high molecular weight
536 C compounds, they may play an important role in degrading woodchips and providing labile C,
537 which can enhance denitrification (Roser et al., 2018). *Cellulomonas* sp. strain WB94 was also
538 detected in the beds other than BioAug beds. This is not surprising because strain WB94 was
539 isolated from the woodchips collected in 2014 from the same site used in this study (Jang et al.,
540 2019). They might have survived in the woodchips and then grew in response to the
541 denitrification-inducing conditions (e.g., low DO, high nitrate, high C).

542 The abundance of *Microvirgula aerodenitrificans* strain BE2.4 also increased after the
543 inoculation in both Fall 2017 and Spring 2018. However, the increase was short lived, and the
544 strain abundance became the background level 42 days after the inoculation. This is consistent
545 with the short-lived increase in NRR in the BioAug beds after the strain inoculation. The short-
546 lived effects may be due to the washout of the inoculated strains from the reactor beds. We also
547 noticed the large variation in the bacteria abundance. This might be related to the heterogeneous
548 distribution of bacteria in the denitrification beds. The method of bacteria inoculation needs to be
549 improved in the future to better retain and distribute bacterial cells in the reactor beds.

550 In addition to nitrate-N, our field-scale woodchip bioreactor also removed TP. The BioStim beds
551 had greater removal of TP in Fall 2017, suggesting that the removal of TP could be associated
552 with microbial activities. However, greater TP removal in the BioStim beds was not seen in
553 Spring 2017, indicating that other factors such as temperature and flow could also influence the
554 removal of TP. Our finding of consistent removal of TP supports previous results of others
555 operating beds at a constant flow rate. Warneke et al. (2011) reported that a woodchip bioreactor
556 treating hydroponic effluent with high TP and DRP concentrations generally removed P,
557 although there were periods of P release as well as capture. Sharrer et al. (2016) found that a

pilot-scale woodchip bioreactor treating aquaculture effluent at a 12-h HRT removed 15% of TP loading over the first 165 days of operation, while 24, 42, and 55-h HRT treatments demonstrated increasing TP removal rates. These studies were conducted on woodchips at the beginning of their service life. Contrary to the previous two shorter-term, constant-flow studies, David et al. (2016) documented much larger bioreactor TP outputs than inputs (also dissolved reactive P) for crop land tile drainage in the second and third years (first year unreported). Thus, there is a need to understand P sink/source dynamics of field bioreactors as beds mature and to test designs that maintain a constant flow rate or prevent abrupt changes to flow rate.

Results from the Spring 2018 campaign were negatively affected by bioclogging of the BioStim treatment; little C was added to the inflow and consequently NRRs were not improved over the non-dosed treatments. Because of the lack of C dosing in Spring 2018, we have not shown nitrate-N port concentration data. Nitrate-N removal results for the Control beds, 5 and 8, may have been influenced by a higher water table in June 2018, particularly 8, which was situated at the end and lowest elevation (See inflow temperature profile, Fig. S3). These challenges are typical of working in the field–in this case on a working farm–under real-world conditions.

4.1 Conclusions

Bioaugmentation showed some promise for enhancing nitrate removal in woodchip bioreactors; however, additional research needs to focus on inoculation procedure and viability of the microbial community over time. Biostimulation has potential to significantly increase nitrate removal rates in woodchip bioreactors; promising results previously seen in the laboratory were confirmed. Additional work is needed to identify an optimum and economical C source and to overcome bioclogging. We conclude that biostimulation demonstrated greater potential than

bioaugmentation in this study, and that both methods need improvement before widespread adoption is recommended.

Declaration of Competing Interest

The authors declare that there are no competing interests.

Acknowledgments

We acknowledge and thank Ed Dorsey, Scott Schumacher, Todd Schumacher; Drs. Laura Christianson, Andry Ranaivoson, and Chanlan Chun; and a host of staff and students too numerous to mention.

Funding was received from: MnDRIVE Environment Initiative, Minnesota Department of Agriculture (Project No. 108837); Minnesota Agricultural Water Resource Center/Discovery Farms Minnesota; University of Minnesota Department of Soil, Water, and Climate; and USDA-ARS. E.L.A. was partly supported by the USDA North Central Region Sustainable Agriculture Research and Education Graduate Student Grant Program.

References

Addy, K., Gold, A. J., Christianson, L. E., David, M. B., Schipper, L. A., & Ratigan, N. A. (2016). Denitrifying Bioreactors for Nitrate Removal: A Meta-Analysis. J Environ Qual, 45(3), 873-881. https://doi.org/10.2134/jeq2015.07.0399.

Anderson, E. L., Jang, J., Venterea, R. T., Feyereisen, G. W., & Ishii, S. (2020). Isolation and characterization of denitrifiers from woodchip bioreactors for bioaugmentation application. J Appl Microbiol, 129(3), 590-600. https://doi.org/10.1111/jam.14655

Bachand, P. A. M., & Horne, A. J. (2000). Denitrification in constructed free-water surface wetlands: II. Effects of vegetation and temperature. Ecological Engineering, 14(1-2), 17-32.

Cao, Y., Li, Y., Ren, L., Sha, M., Lv, D., Wang, S., & Kong, F. (2021). Bio-clogging mitigation in vertical subsurface flow constructed wetlands using rhamnolipids-citric acid compound. Chemical Engineering Journal, 426. https://doi.org/10.1016/j.cej.2021.131278

Christianson, L. E., Cooke, R. A., Hay, C. H., Helmers, M. J., Feyereisen, G. W., Ranaivoson, A. Z., McMaine, J. T., McDaniel, R., Rosen, T. R., Pluer, W. T., Schipper, L. A., Dougherty, H., Robinson, R. J., Layden, I. A., Irvine-Brown, S. M., Manca, F., Dhaese, K., Nelissen, V., & von Ahnen, M. (2021). Effectiveness of Denitrifying Bioreactors on Water Pollutant Reduction from Agricultural Areas. Transactions of the ASABE, 64(2), 641-658. https://doi.org/10.13031/trans.14011

Christianson, L., Bhandari, A., Helmers, M., Kult, K., Sutphin, T., & Wolf, R. (2012). Performance Evaluation of Four Field-Scale Agricultural Drainage Denitrification Bioreactors in Iowa. Transactions of the ASABE, 55(6), 2163-2174. <Go to ISI>://WOS:000313998700013.

Clesceri, L.S., Greenburg, A.E., & D.A. Eaton, D.A. (eds.). (1998). Standard Methods for the Examination of Water and Wastewater. 20th ed. Am. Public Health Assoc., Washington, DC.

Crumpton, W. G. (2001). Using wetlands for water quality improvement in agricultural watersheds; the importance of a watershed scale approach. Water Science and Technology, 44(11-12), 559-564. https://doi.org/DOI 10.2166/wst.2001.0880

David, M. B., Gentry, L. E., Cooke, R. A., & Herbstritt, S. M. (2016). Temperature and Substrate Control Woodchip Bioreactor Performance in Reducing Tile Nitrate Loads in East-Central Illinois. Journal of Environmental Quality, 45(3), 822-829. https://doi.org/10.2134/jeq2015.06.0296

Ghane, E., Feyereisen, G. W., & Rosen, C. J. (2016). Non-linear hydraulic properties of woodchips necessary to design denitrification beds. Journal of Hydrology, 542, 463-473. https://doi.org/10.1016/j.jhydrol.2016.09.021

Ghane, E., Feyereisen, G. W., Rosen, C. J., & Tschirner, U. W. (2018). Carbon Quality of Four-Year-Old Woodchips in a Denitrification Bed Treating Agricultural Drainage Water. Transactions of the ASABE, 61(3), 995-1000. https://doi.org/10.13031/trans.12642

Ghane, E., Feyereisen, G. W., & Rosen, C. J. (2019). Efficacy of bromide tracers for evaluating the hydraulics of denitrification beds treating agricultural drainage water. Journal of Hydrology, 574, 129-137. https://doi.org/10.1016/j.jhydrol.2019.02.031

Guofen, H., Wei, Z., Lianfang, Z., & Yunhui, Z. (2010). Applying solubilization treatment to reverse clogging in laboratory-scale vertical flow constructed wetlands. Water Sci Technol, 61(6), 1479-1487. https://doi.org/10.2166/wst.2010.038

Hoover, N. L., Bhandari, A., Soupir, M. L., & Moorman, T. B. (2016). Woodchip denitrification bioreactors: Impact of temperature and hydraulic retention time on nitrate removal. Journal of Environmental Quality, 45(3), 803-812. https://doi.org/10.2134/jeq2015.03.0161

Feyereisen, G. W., Moorman, T. B., Christianson, L. E., Venterea, R. T., Coulter, J. A., & Tschirner, U. W. (2016). Performance of Agricultural Residue Media in Laboratory

642 Denitrifying Bioreactors at Low Temperatures. J Environ Qual, 45(3), 779-787.
643 https://doi.org/10.2134/jeq2015.07.0407.
644 Jang, J., Anderson, E. L., Venterea, R. T., Sadowsky, M. J., Rosen, C. J., Feyereisen, G. W., &
645 Ishii, S. (2019). Denitrifying Bacteria Active in Woodchip Bioreactors at Low-Temperature
646 Conditions. Front Microbiol, 10, 635. https://doi.org/10.3389/fmicb.2019.00635
647 Jeglot, A., Miranda-Velez, J. F., Plauborg, F., & Elsgaard, L. (2022a). Nitrate removal and
648 environmental side-effects controlled by hydraulic residence time in woodchip bioreactors
649 treating cold agricultural drainage water. Environmental Technology.
650 https://doi.org/10.1080/09593330.2022.2091482
651 Jeglot, A., Schnorr, K. M., Sorensen, S. R., & Elsgaard, L. (2022b). Isolation and
652 characterization of psychrotolerant denitrifying bacteria for improvement of nitrate removal
653 in woodchip bioreactors treating agricultural drainage water at low temperature.
654 Environmental Science-Water Research & Technology, 8(2), 396-406.
655 https://doi.org/10.1039/d1ew00746g
656 Hites, R. A. (2019). Correcting for Censored Environmental Measurements. Environ Sci
657 Technol, 53(19), 11059-11060. https://doi.org/10.1021/acs.est.9b05042
658 Ishii, S., Segawa, T., & Okabe, S. (2013). Simultaneous quantification of multiple food- and
659 waterborne pathogens by use of microfluidic quantitative PCR. Appl Environ Microbiol,
660 79(9), 2891-2898. https://doi.org/10.1128/AEM.00205-13
661 Manca, F., De Rosa, D., Reading, L. P., Rowlings, D. W., Scheer, C., Layden, I., Irvine-Brown,
662 S., Schipper, L. A., & Grace, P. R. (2020). Nitrate removal and greenhouse gas production
663 of woodchip denitrification walls under a humid subtropical climate. Ecological

664 Engineering, 156. https://doi.org/ARTN 105988
665 10.1016/j.ecoleng.2020.105988
666 Maxwell, B. M., Birgand, F., Schipper, L. A., Christianson, L. E., Tian, S., Helmers, M. J.,
667 Williams, D. J., Chescheir, G. M., & Youssef, M. A. (2019). Drying-Rewetting Cycles
668 Affect Nitrate Removal Rates in Woodchip Bioreactors. J Environ Qual, 48(1), 93-101.
669 https://doi.org/10.2134/jeq2018.05.0199
670 McDowell, R. W., Noble, A., Pletnyakov, P., & Mosley, L. M. (2021). Global database of
671 diffuse riverine nitrogen and phosphorus loads and yields. Geoscience Data Journal, 8(2),
672 132-143. https://doi.org/10.1002/gdj3.111
673 Nivala, J., Knowles, P., Dotro, G., Garcia, J., & Wallace, S. (2012). Clogging in subsurface-flow
674 treatment wetlands: measurement, modeling and management. Water Res, 46(6), 1625-
675 1640. https://doi.org/10.1016/j.watres.2011.12.051
676 Nordstrom, A., & Herbert, R. B. (2017). Denitrification in a low-temperature bioreactor system
677 at two different hydraulic residence times: laboratory column studies. Environmental
678 Technology, 38(11), 1362-1375. https://doi.org/10.1080/09593330.2016.1228699
679 Patton, C.J., & J.R. Kryskalla, J.R. (2003). Methods of analysis by the U.S. Geological Survey
680 National Water Quality Laboratory: Evaluation of alkaline persulfate digestion as an
681 alternative to Kjeldahl digestion for the determination of total and dissolved nitrogen and
682 phosphorus in water. Water Resources Investigations Rep. 03-4174. Denver, CO: Branch of
683 Information Services, United States Geological Survey.
684 Ping, T., Zeshun, X., Yongchao, Z., & Yiping, Z. (2018). Enzyme treatment improves the
685 performance of laboratory-scale vertical flow constructed wetland. Bioresour Technol, 268,
686 665-671. https://doi.org/10.1016/j.biortech.2018.08.048

687 Roser, M. B., Feyereisen, G. W., Spokas, K. A., Mulla, D. J., Strock, J. S., & Gutknecht, J.
688 (2018). Carbon Dosing Increases Nitrate Removal Rates in Denitrifying Bioreactors at Low-
689 Temperature High-Flow Conditions. Journal of Environmental Quality, 47(4), 856-864.
690 https://doi.org/10.2134/jeq2018.02.0082

691 SAS Institute. (2016). The SAS system for Windows. Version 9.4. SAS Inst., Cary, NC.

692 Schipper, L. A., Robertson, W. D., Gold, A. J., Jaynes, D. B., & Cameron, S. C. (2010).
693 Denitrifying bioreactors-An approach for reducing nitrate loads to receiving waters.
694 Ecological Engineering, 36(11), 1532-1543. https://doi.org/10.1016/j.ecoleng.2010.04.008

695 Sharrer, K. L., Christianson, L. E., Lepine, C., & Summerfelt, S. T. (2016). Modeling and
696 mitigation of denitrification 'woodchip' bioreactor phosphorus releases during treatment of
697 aquaculture wastewater. Ecological Engineering, 93, 135-143.
698 https://doi.org/10.1016/j.ecoleng.2016.05.019

699 Shi, Y., Huang, J., Zeng, G., Gu, Y., Chen, Y., Hu, Y., Tang, B., Zhou, J., Yang, Y., & Shi, L.
700 (2017). Exploiting extracellular polymeric substances (EPS) controlling strategies for
701 performance enhancement of biological wastewater treatments: An overview. Chemosphere,
702 180, 396-411. https://doi.org/10.1016/j.chemosphere.2017.04.042

703 Song, X., Ding, Y., Wang, Y., Wang, W., Wang, G., & Zhou, B. (2015). Comparative study of
704 nitrogen removal and bio-film clogging for three filter media packing strategies in vertical
705 flow constructed wetlands. Ecological Engineering, 74, 1-7.
706 https://doi.org/10.1016/j.ecoleng.2014.08.008

707 Suliman, F., French, H. K., Haugen, L. E., & Søvik, A. K. (2006). Change in flow and transport
708 patterns in horizontal subsurface flow constructed wetlands as a result of biological growth.
709 Ecological Engineering, 27(2), 124-133. https://doi.org/10.1016/j.ecoleng.2005.12.007

Timmermans, P., & Vanhaute, A. (1983). Denitrification with Methanol - Fundamental-Study of the Growth and Denitrification Capacity of *Hyphomicrobium* Sp. Water Research, 17(10), 1249-1255. https://doi.org/Doi 10.1016/0043-1354(83)90249-X

Tyagi, M., da Fonseca, M. M., & de Carvalho, C. C. (2011). Bioaugmentation and biostimulation strategies to improve the effectiveness of bioremediation processes. Biodegradation, 22(2), 231-241. https://doi.org/10.1007/s10532-010-9394-4

Wang, H., Feyereisen, G.W., Wang, P., Rosen, C.J., Sadowsky, M.J., & Ishii, S. (202#). Impacts of biostimulation and bioaugmentation on woodchip bioreactor microbiomes. (in preparation).

Warneke, S., Schipper, L. A., Bruesewitz, D. A., McDonald, I., & Cameron, S. (2011). Rates, controls and potential adverse effects of nitrate removal in a denitrification bed. Ecological Engineering, 37(3), 511-522. https://doi.org/10.1016/j.ecoleng.2010.12.006

Tables and Figures for Main Document

Table 1. Automated sample outflow concentrations for nitrate-N, ammonium-N, and TP by treatment, nitrate-N and TP load reduction in percent, and nitrate removal rate (NRR) by treatment. Sampling interval for Fall 2016 was 1 day, for Spring 2017 and Fall 2017 was 3 days, and for Spring 2018 was 2 days.

	Treatment		
Campaign	Control	BioAug	BioStim
	Outflow Nitrate-N Concentration (mg N L^{-1})		
Fall 2016	14.4	14.9	14.9
Spring 2017	14.7 a†	13.9 a	5.9 b
Fall 2017	11.6 a	12.1 a	10.1 b
Spring 2018	9.8 c	11.0 b	11.9 c
	Nitrate-N Load Reduction (%)		
Fall 2016	25.8	23.2	22.8
Spring 2017	17.5 b	21.2 b	65.5 a
Fall 2017	20.0 b	16.4 b	30.6 a
Spring 2018	27.5 a	19.5 b	13.3 c
	NRR (g N m-3 d-1)		
Fall 2016	5.90	6.65	6.40
Spring 2017	4.38 b	5.81 b	15.01 a
Fall 2017	4.14 b	3.88 b	5.56 a
Spring 2018	4.93	4.09	4.86
	Outflow Ammonium-N Concentration (mg N L^{-1})		
Fall 2016	n/a ‡	n/a	n/a
Spring 2017	0.16	0.21	0.12
Fall 2017	0.07	0.06	0.06
Spring 2018	0.04	0.04	0.03
	Outflow Total-P Concentration (mg P L^{-1})		
Fall 2016	0.027	0.021	0.018
Spring 2017	0.035	0.034	0.026
Fall 2017	0.021 a	0.019 a	0.014 b
Spring 2018	0.033	0.036	0.037
	Total-P Load Reduction (%)		

Fall 2016	64.0	71.3	74.7
Spring 2017	58.9	60.3	68.8
Fall 2017	70.6 b	72.9 b	80.4 a
Spring 2018	60.6	57.2	55.5

727 †Values are means. Within a row, means followed by the same lowercase letter are not

728 significantly different a $P \leq 0.10$.

729 ‡ n/a denotes that Fall 2016 ammonium-N data are not available.

730 Table 2. Weekly outflow DOC concentrations averaged across treatments for Spring 2017, Fall
731 2017, and Spring 2018. Delta-DOC represents the average outflow DOC concentration across
732 treatments minus the inlet tank DOC concentration; thus, a (+) value represents net DOC export
733 and a (–) value represents net DOC consumption.

Sampling Campaign	Sampling Dates	Avg. outflow DOC concentration (mg C L^{-1})	Delta-DOC concentration (mg C L^{-1})
Spring 2017	11 May 2017	11.0	6.3 A
	18 May 2017	3.9	-0.6
	24 May 2017	5.8	0.5
	31 May 2017	5.4	0.1
	7 Jun 2017	5.4	1.0
	15 Jun 2017	5.9	2.9
	21 Jun 2017	6.4	-0.2
	29 Jun 2017	6.7	-0.3
	7 Jul 2017	6.2	0.4
Fall 2017	7 Nov 2017	5.3 bc†	0.3 A
	20 Nov 2017	5.7 a	0.4 A
	29 Nov 2017	5.6 ab	0.5 A
	4 Dec 2017	5.2 c	0.4 A
Spring 2018	7 May 2018	5.2 c	0.2
	5 June 2018	6.2 b	1.3 A
	30 June 2018	7.5 a	0.5 A

734 † Weekly DOC mean concentrations followed by the same lowercase letter for the Fall 2017
735 sampling dates are not significantly different at $P \leq 0.10$. There are no significant differences
736 among dates for Spring 2017. Sampling dates in the Delta-DOC column followed by an
737 uppercase "A" are significantly different than zero at $P \leq 0.10$.

738 **Figures**

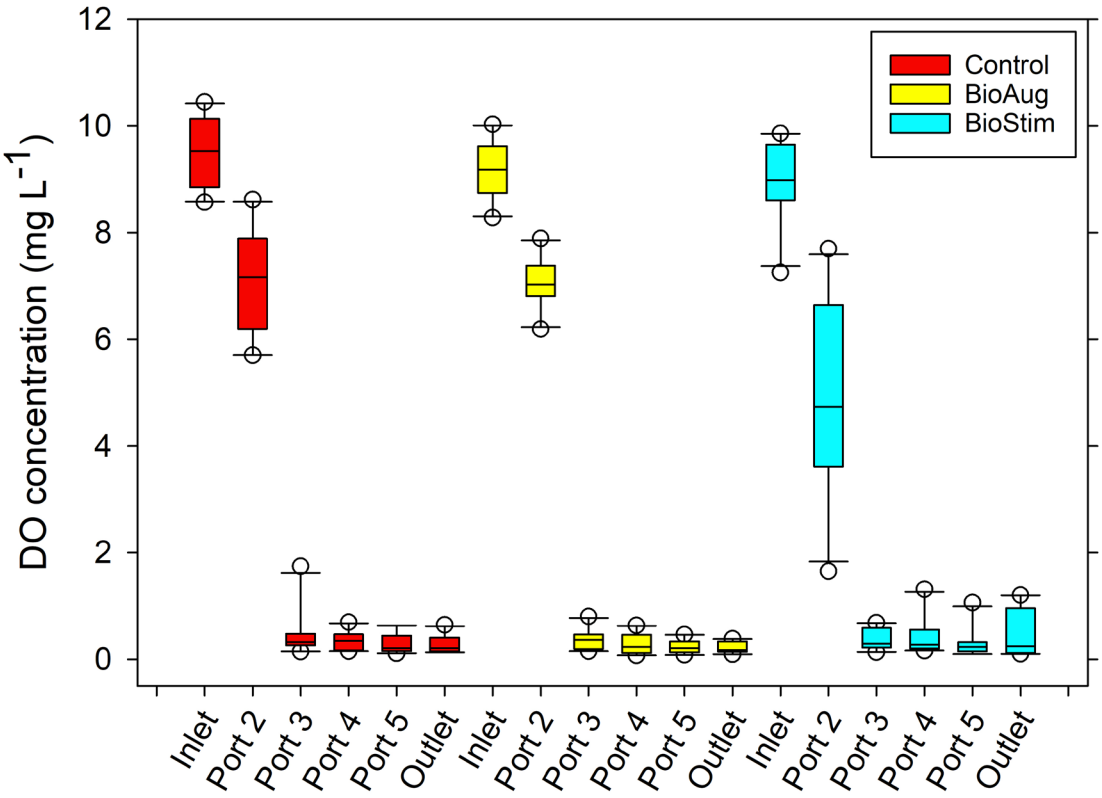

Fig. 1. Dissolved oxygen (DO) concentrations at the inlets/outlets and ports along the bioreactor beds for the Control, BioAug, and BioStim treatments. The data represent five sampling dates during the Spring 2017 (2) and Fall 2017 (3) campaigns.

739

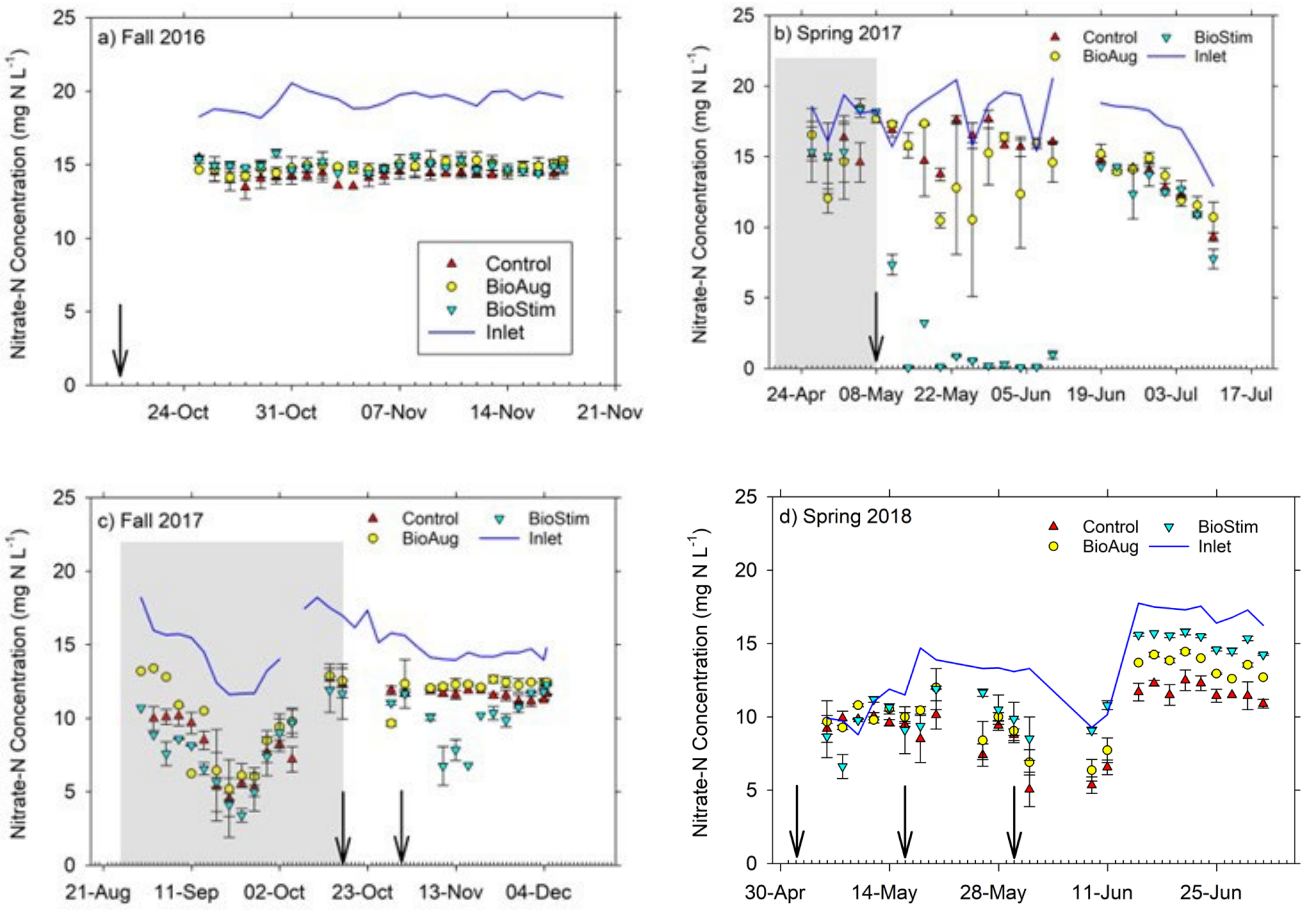

Fig. 2. Nitrate-N concentrations for a) Fall 2016, b) Spring 2017, and c) Fall 2017. Treatment data are averages; error bars denote standard errors (n = 2). Arrows indicate dates of inoculation and beginning of acetate dosing. Shaded area indicates pre-inoculation/pre-dosing period. A 63-mm precipitation event occurred on 11 June 2018.

740

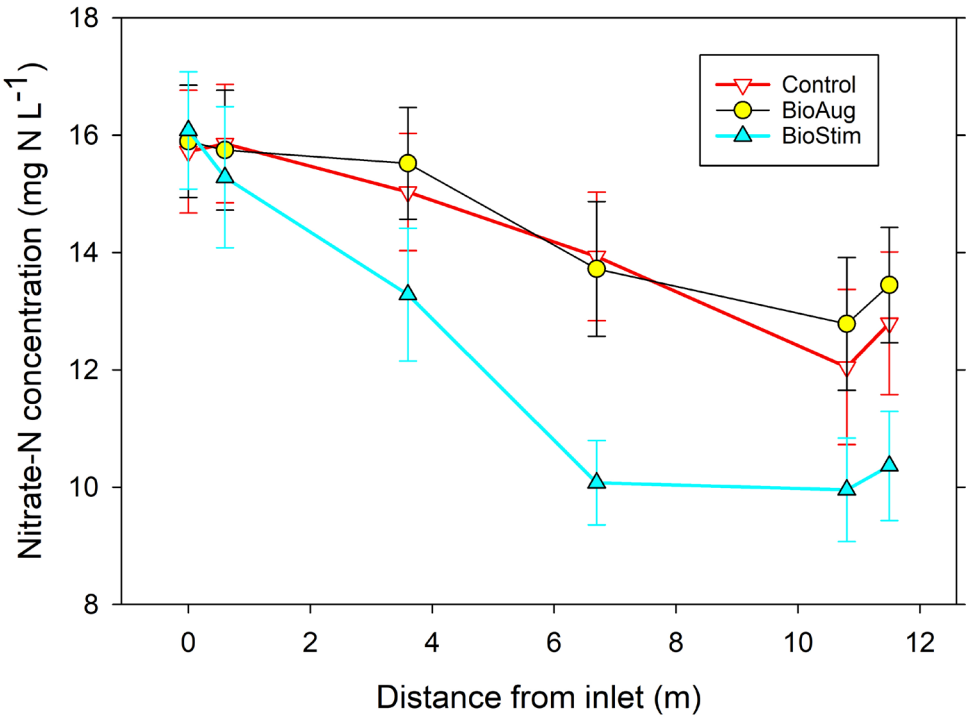

Fig. 3. Nitrate-N concentrations at the inlets/outlets and ports along the bioreactor beds for the Control, BioAug, and BioStim treatments. The data represent four sampling dates after treatment initiation in Spring 2017 (1) and Fall 2017 (3) campaigns.

741

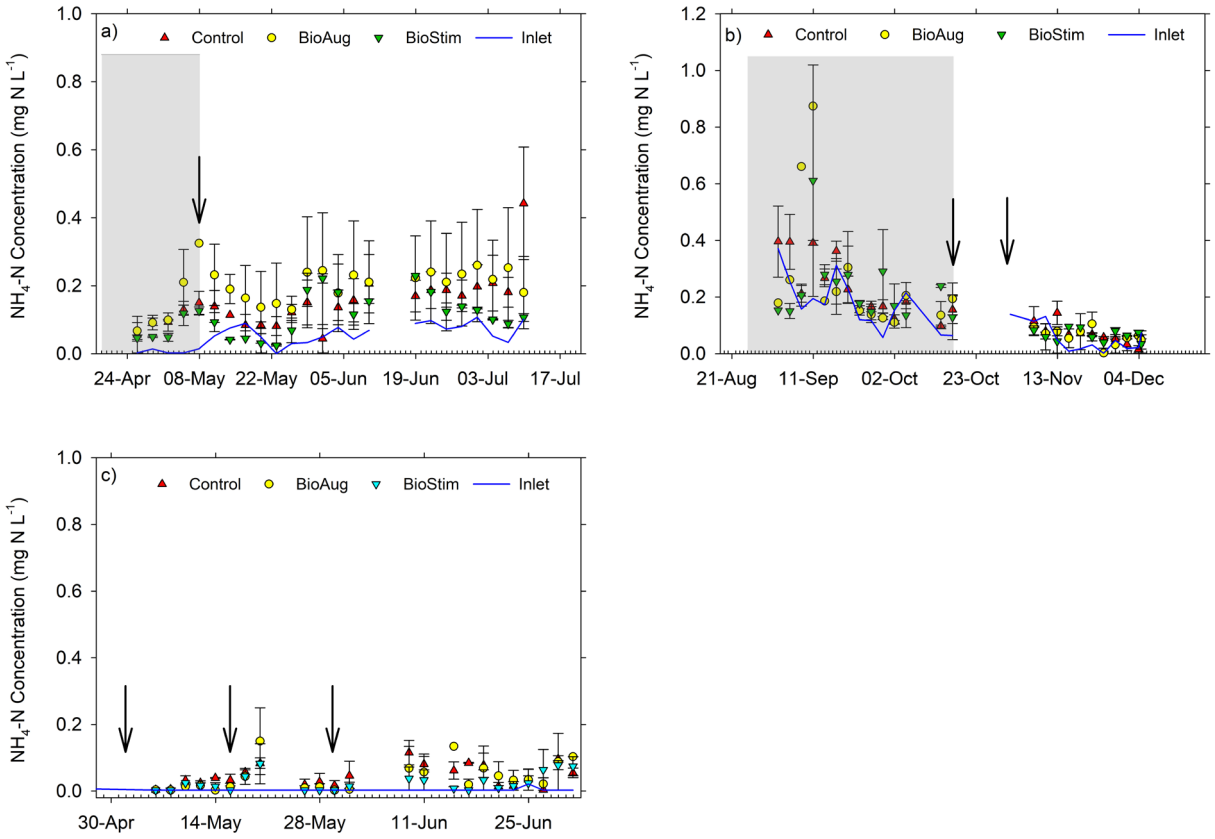

Fig. 4. Ammonium-N concentrations for a) Spring 2017, and b) Fall 2017. Treatment data are averages; error bars denote standard errors (n = 2). Arrows indicate dates of inoculation and beginning of acetate dosing. Shaded area indicates pre-inoculation/pre-dosing period.

742

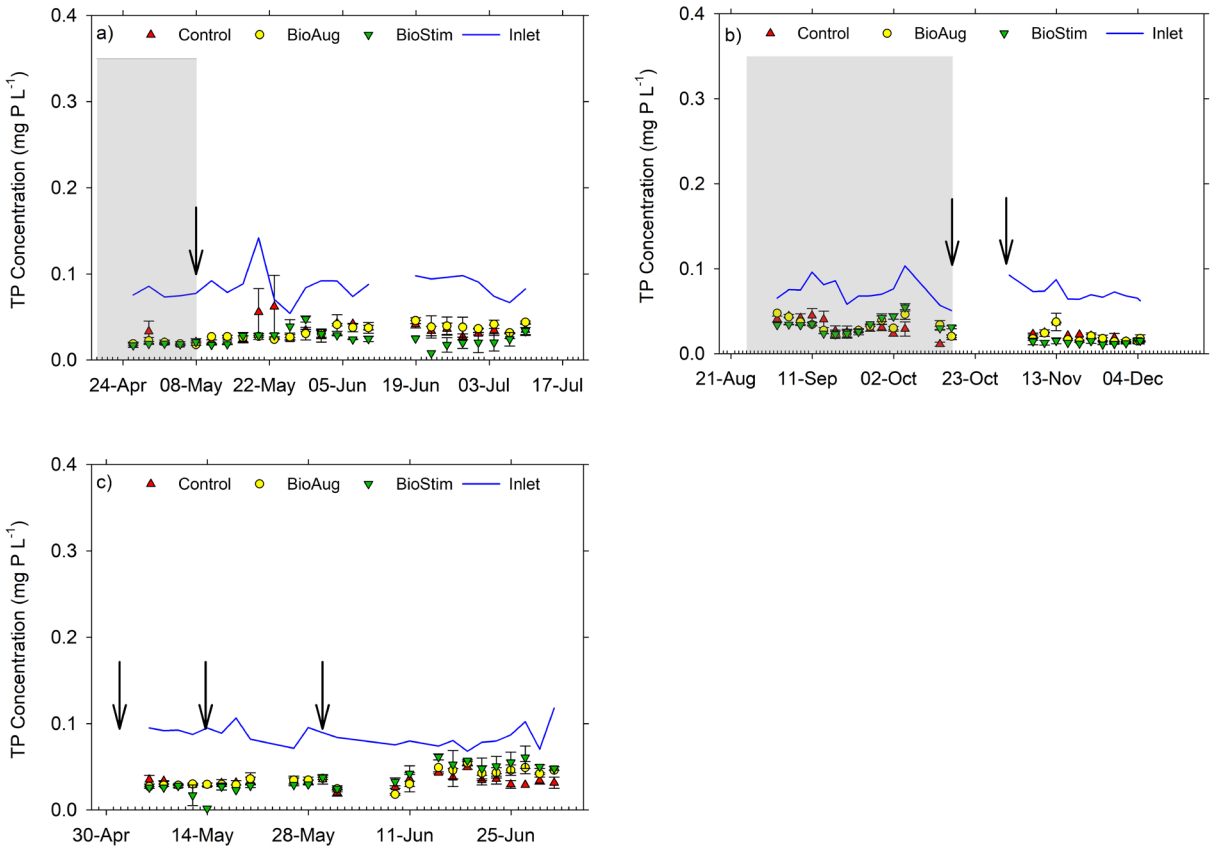

Fig. 5. Total-P concentrations for a) Spring 2017, b) Fall 2017, and c) Spring 2018. Treatment data are averages; error bars denote standard errors (n = 2). Arrows indicate dates of inoculation and beginning of acetate dosing. Shaded area indicates pre-inoculation/pre-dosing period. The data gap in Fall 2017 occurred due to a bed flow pumping rate mistake after the first inoculation and freezing conditions that interrupted the experiment while anti-freeze provisions were put in place.

743

Supplementary Material

Carbon supplementation and bioaugmentation to improve denitrifying woodchip bioreactor performance under cold conditions

Gary W. Feyereisen*[1]
Hao Wang[2]
Ping Wang[3]
Emily L. Anderson[2]
Jeonghwan Jang[4]
Ehsan Ghane[5]
Jeffrey A. Coulter[6]
Carl J. Rosen[2]
Michael J. Sadowsky[2,3]
Satoshi Ishii[2,3]

*Corresponding Author: gary.feyereisen@usda.gov

[1] USDA-ARS Soil and Water Management Research Unit, 1991 Upper Buford Circle, 439 Borlaug Hall, St. Paul, MN 55108, USA.
[2] Department of Soil, Water, and Climate, University of Minnesota, 1991 Upper Buford Circle, 439 Borlaug Hall, St. Paul, MN 55108, USA.
[3] BioTechnology Institute, University of Minnesota, 140 Gortner Lab, 1479 Gortner Ave., St. Paul, MN 55108, USA.
[4] Division of Biotechnology, Jeonbuk National University, 79 Gobong-ro, Iksan-si, Jeollabuk-do, 54596, Republic of Korea.
[5] Department of Biosystems and Agricultural Engineering, Michigan State University, 524 S. Shaw Lane, 206 Farrall Hall, East Lansing, MI 48824, USA.
[6] Department of Agronomy and Plant Genetics, University of Minnesota, 1991 Upper Buford Circle, 411 Borlaug Hall, St. Paul, MN 55108, USA.

Materials and Methods–Additional Details

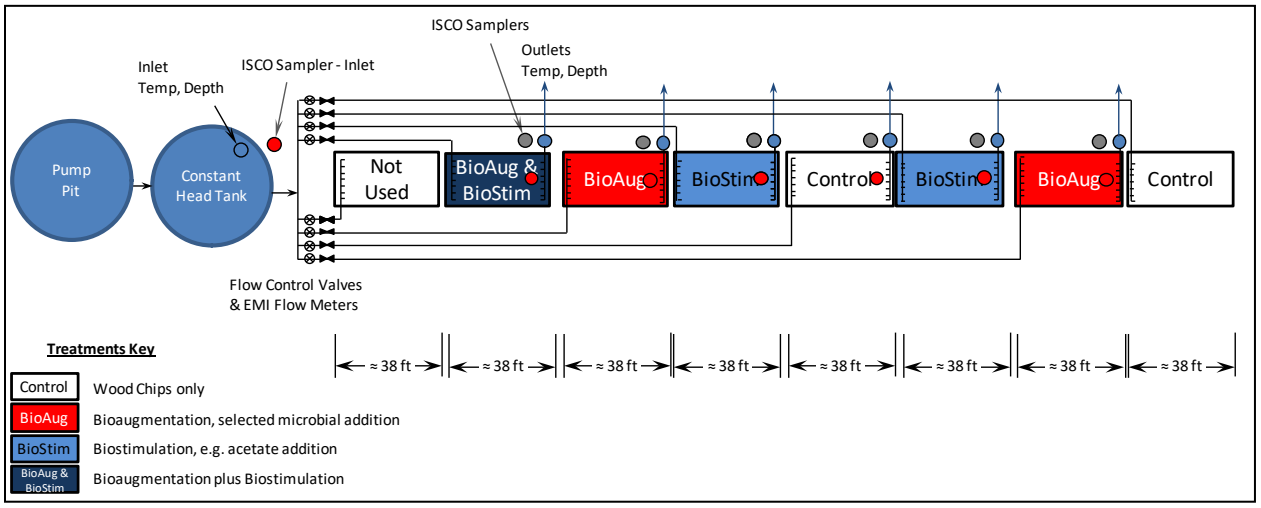

Fig. S1. Schematic of replicated bioreactor beds. Treatments represented were for 2017 and 2018.

Fig. S2. Port baskets containing woodchip balls.

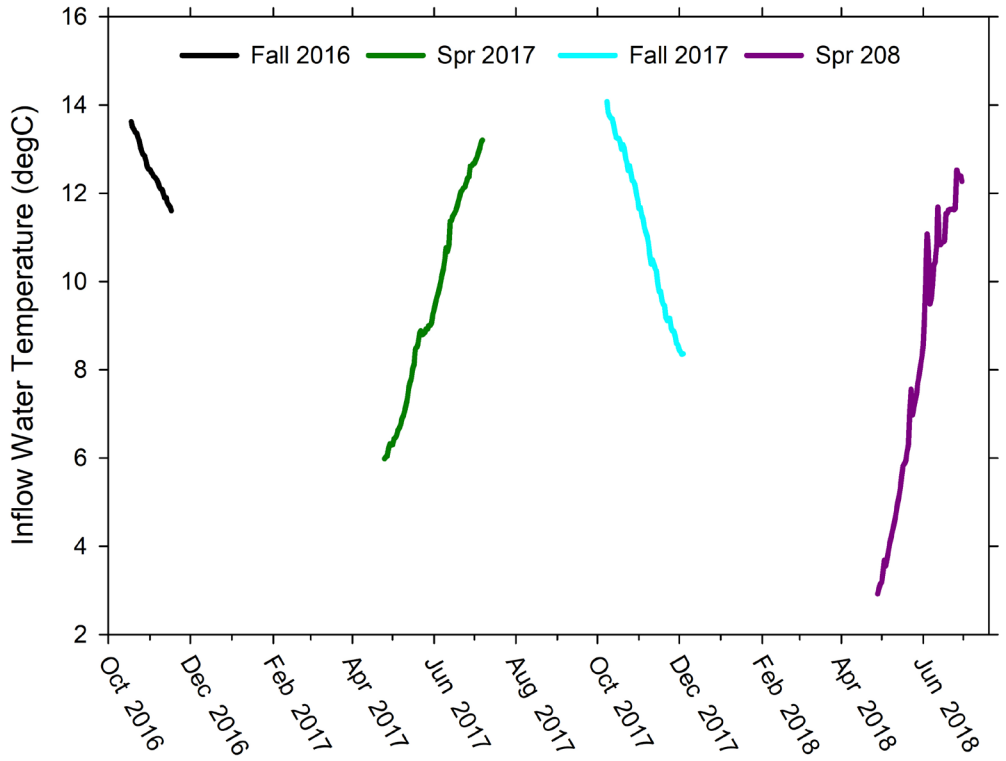

Fig. S3. Average daily inflow temperatures during the four experimental campaigns. The upward spikes during the Spring 2018 campaign (far right) reflect the effect of large precipitation events, which tended to influence water table height at the site.

777

778

779 Table S1. Inoculation dates and inoculants. † Dates after inoculation and addition of acetate that
780 were included in port water sample analyses.

Sampling Dates	Inoculant	OD600
20 October 2016	*Bacillus pseudomycoides* I32.	n/a
27 October 2016	n/a	n/a
8 May 2017	*Cellulomonas* sp. strain WB94	No Measurement
†15 May 2017	n/a	No Measurement
23 June 2017	n/a	No Measurement
17 October 2017	*Microvirgula* sp. strain BE2.4, *Lelliottia* sp. strain BB2.1	BE2.4: 0.097; BB2.1: 0.0469
†31 October 2017	*Microvirgula* sp. strain BE2.4, *Lelliottia* sp. strain BB2.1	1.0798
†14 November 2017	n/a	No Measurement
†28 November 2017	n/a	No Measurement
2 May 2018	*Microvirgula* sp. Strain BE2.4	0.642
16 May 2018	*Microvirgula* sp. Strain BE2.4	0.761
30 May 2018	*Microvirgula* sp. Strain BE2.4; *Cellulomonas* sp. Strain WB94	BE2.4: 0.537; WB94: 0.325

781

782 Table S2. Acetate concentrations and C:N ratios from Fall 2016 through Spring 2018.

	October 2016	May 2017	July 2017	October 2017	November 2017	Spring 2018
Acetate-C Conc (mg C L^{-1})	2,770	28,500	27,900	6,050	9,940	19,210
Acetate Pumping Rate (mL/min)	200	200	200	13	8	13
Duty Cycle # cycles, timing length of each cycle	5 min on, 10 min off for 1 hr each 8 hrs	21 sec each 5 min 7%	†21 sec each 5 min 7%	†100%	†100%	†100%
Design NO_3-N Concentration (mg N L^{-1})	19	22	14	15	16	16
Design Bed Flow Rate (gal/min)	2.5	2.5	2.5	2.7	2.7	7.5
Design C:N (mole C:mole N	0.15	2.52	1.00	0.60	0.57	0.64

783 †Pump controlled by water level in inlet pipe. When the water level rose in the inlet pipe, indicating bioclogging, pumping of acetate

784 ceased until the level reduced.

785 Table S3. Weekly manual sampling dates for the Spring 2017, Fall 2017, and Spring 2018
786 campaigns for DOC analysis

Weekly Sampling Dates Spring 2017	**Weekly Sampling Dates Fall 2017**	**Weekly Sampling Dates Spring 2018**
11 May 2017	17 October 2017	7 May 2018
18 May 2017	25 October 2017	5 June 2018
24 May 2017	7 November 2017	30 June 2018
31 May 2017	20 November 2017	
7 June 2017	29 November 2017	
15 June 2017	4 December 2017	
21 June 2017		
29 June 2017		
7 July 2017		

787

788

789

790 Table S4. Primer and probe sequences for inoculants.

Strain	*Forward Primer*	*Reverse Primer*	*Probe*
BE2.4	5'-CTGCATGCGGGATACCTT-3'	5'-CTGAGCAGGGACCTCCTTTT-3'	Universal probe #113 (Roche)
WB94	5'-CCTGTGGTCGGTGGTTGT-3'	5'-ATCAGCGCAGACCAGCTC-3'	Universal probe #83 (Roche)

791

Table S5. Dates that automated samples were collected for the Fall 2016, Spring 2017, Fall 2017, and Spring 2018 campaigns.

Fall 2016	Spring 2017	Fall 2017	Spring 2018
24 October 2016	10 May 2017	28 October 2017	5 May 2018
25 October 2016	13 May 2017	31 October 2017	7 May 2018
26 October 2016	16 May 2017	‡	9 May 2018
27 October 2016	19 May 2017	6 November 2017	11 May 2018
28 October 2016	22 May 2017	9 November 2017	13 May 2018
29 October 2016	25 May 2017	12 November 2017	15 May 2018
30 October 2016	28 May 2017	15 November 2017	17 May 2018
31 October 2016	31 May 2017	18 November 2017	19 May 2018
1 November 2016	3 June 2017	21 November 2017	§
2 November 2016	6 June 2017	24 November 2017	25 May 2018
3 November 2016	9 June 2017	27 November 2017	27 May 2018
4 November 2016	†	30 November 2017	29 May 2018
5 November 2016	†	3 December 2017	31 May 2018
6 November 2016	18 June 2017	4 December 2017	§
7 November 2016	21 June 2017		§
8 November 2016	24 June 2017		§
9 November 2016	27 June 2017		8 Jun 2018
10 November 2016	30 June 2017		10 Jun 2018
11 November 2016	3 July 2017		§
12 November 2016	6 July 2017		14 Jun 2018
13 November 2016	9 July 2017		16 Jun 2018
14 November 2016			18 Jun 2018
15 November 2016			20 Jun 2018
16 November 2016			22 Jun 2018
17 November 2016			24 Jun 2018
			26 Jun 2018
			28 Jun 2018
			30 Jun 2018

† Dates missed due to bioclogging.

‡ Date missed while bioreactor equipment and sensors were being winterized.

§ Dates excluded due to pumping issues.

Results and Discussion–Additional Details

Table S6. Actual hydraulic retention times (AHRT) by treatment for the Fall 2016, Spring 2017, and Fall 2017 campaigns.

Treatment	Mean AHRT			
	Fall 2016	Spring 2017	Fall 2017	Spring 2018
	---------- (h) ----------			
Control	11.7 a†	10.2 a	10.0 a	11.5 a
BioAug	9.8 a	11.1 a	10.1 a	11.0 a
BioStim	10.7 a	11.2 a	11.2 a	5.2 b

† Means followed by the same lowercase letter within a column are not significantly different at $P \leq 0.1$.

803 Table S7. Average outflow Delta_NH4-N concentrations (outflow minus inflow) across
804 treatments for Spring 2017 and Fall 2017. P-values indicate probability that Delta-NH4-N is
805 different from zero for a given date.

Sampling Campaign	Sampling Dates	Delta-NH4-N concentration (mg NH_4-N L-1)	p-value for different from zero
Spring 2017	10 May 2017	0.102	0.043†
	13 May 2017	0.043	0.411
	16 May 2017	0.008	0.878
	19 May 2017	0.034	0.486
	22 May 2017	0.084	0.093†
	25 May 2017	0.077	0.125
	28 May 2017	0.160	0.002†
	31 May 2017	0.120	0.018†
	03 Jun 2017	0.088	0.080†
	06 Jun 2017	0.125	0.014†
	09 Jun 2017	0.122	0.017†
	18 Jun 2017	0.114	0.032†
	21 Jun 2017	0.101	0.057†
	24 Jun 2017	0.101	0.045†
	27 Jun 2017	0.101	0.045†
	30 Jun 2017	0.088	0.080†
	03 Jul 2017	0.124	0.015†
	06 Jul 2017	0.141	0.006†
	09 Jul 2017	0.141	0.006†
Fall 2017	06 Nov 2017	-0.017	0.043†
	09 Nov 2017	-0.062	0.411
	12 Nov 2017	0.041	0.878
	15 Nov 2017	0.065	0.486
	18 Nov 2017	0.060	0.093†
	21 Nov 2017	0.046	0.125
	24 Nov 2017	0.031	0.002†
	27 Nov 2017	0.008	0.018†
	30 Nov 2017	0.033	0.080†
	03 Dec 2017	0.029	0.014†
	04 Dec 2017	-0.026	0.017†
Spring 2018	5 May 18	0.001	0.967
	7 May 18	0.001	0.954
	9 May 18	0.017	0.403
	11 May 18	0.019	0.358
	13 May 18	0.016	0.373

15 May 18	0.014	0.452
17 May 18	0.050	0.014†
19 May 18	0.103	<0.001†
25 May 18	0.008	0.665
27 May 18	0.012	0.519
29 May 18	0.005	0.789
31 May 18	0.019	0.287
8 Jun 18	0.071	<0.001†
10 Jun 18	0.054	0.004†
14 Jun 18	0.056	0.007†
16 Jun 18	0.033	0.072†
18 Jun 18	0.057	0.002†
20 Jun 18	0.020	0.261
22 Jun 18	0.019	0.306
24 Jun 18	0.011	0.575
26 Jun 18	0.018	0.427
28 Jun 18	0.085	<0.001†
30 Jun 18	0.058	0.005†

† Dates for which $P \leq 0.10$.

Table S8. Average weekly outflow Delta-DOC concentrations (outflow minus inflow) by treatment for Spring 2017 and Fall 2017. P-values indicate probability that Delta-DOC is different from zero.

Campaign	Treatment					
	BioAug		BioStim		Control	
	Delta-DOC Concentration					
	(mg C L^{-1})	p-value	(mg C L^{-1})	p-value	(mg C L^{-1})	p-value
Spring 2017	1.73	0.27	0.26	0.85	1.45	0.36
Fall 2017	0.29	0.21	0.35	0.16	0.59	0.07†
Spring 2018	0.59	0.06†	0.61	0.06†	0.79	0.04†

† Treatment-campaigns for which outflow minus inflow DOC concentrations were greater than zero, indicating net production of DOC ($P \leq 0.10$).